Thermochimica Acta, 229 (1993) 97–109
Elsevier Science Publishers B.V., Amsterdam

Heat losses which cannot be compensated for and their contribution to the temperature dependence of caloric measuring errors in dynamic differential calorimeters [1]

W. Poeßnecker
KAI-e.V., Nürnberger Str. 43, D-01187 Dresden (Germany)
(Received 24 May 1993; accepted 2 June 1993)

Abstract

Because of their sophisticated design, adiabatic calorimeters record the true caloric properties of a substance. In contrast, the compensation of losses and, thus, the quasi-adiabatic behaviour of the more common isoperibolic differential calorimeters is achieved by balancing heat losses.

Based on previously published models, a theory for isoperibolic differential calorimeters is developed which closely follows the actual measuring conditions. In particular, the relation between dynamic and static heat losses is addressed, and the limits for the compensation of losses are indicated.

The investigation has resulted in the recommendation of measuring conditions which, if closely followed for various temperatures, allow the measuring error caused by non-compensated losses to be determined with the help of zero-line offsets, without the necessity of knowing the air gap thicknesses or the heat transfer coefficients that cause the error.

INTRODUCTION

Caloric measuring errors are caused by an undesired heat exchange with the surroundings. Without the expensive design of better devices, even adiabatic calorimeters are characterized by heat losses. Because such apparatus can only be afforded by government institutes and because their realization requires certain minimum size, isoperibolic differential calorimeters are used in practice; here, using small samples, quasi-adiabatic behaviour is approximated by compensating for the losses [1].

However, in the measurement process, complete compensation of losses is not possible [2], and this may introduce measuring errors as a result.

[1] Presented at the Tenth Ulm Conference, Ulm, Germany, 17–19 March 1993.

These measuring errors are theoretically computed under practical conditions, because this is the only way to separate all of the, mostly complex, influencing parameters.

However, in general an experimental determination of the individual influencing parameters is not possible, so that such an error analysis is inevitably only qualitative in nature.

In order to provide quantitative descriptions of the measuring errors without knowing the values of the parameters that lead to those errors, more readily measured parameters are required with which to determine the measuring error.

These studies are designed to minimize incorrect error indications which, because exact physical interrelations are unknown, are mostly intuitive in origin.

PHYSICAL MODEL

The physical model is shown in Fig. 1. The system containing the sample is on the right side and is identified by the index R and the number (2); the left side is the reference system, labeled L and (1). Each system consists of an internal and external part. The right internal part represents the sample and sample pan, whereas the left internal part represents the reference pan only. The left and right external parts are the sample holders with the heating and sensor windings which support the covers of the sample holder and reference holder. The sample and reference holder are enclosed by a casing thermostatted at the temperature T_U; only the upper cover of the block is shown. There is an air gap of thickness d_{1R} between the sample

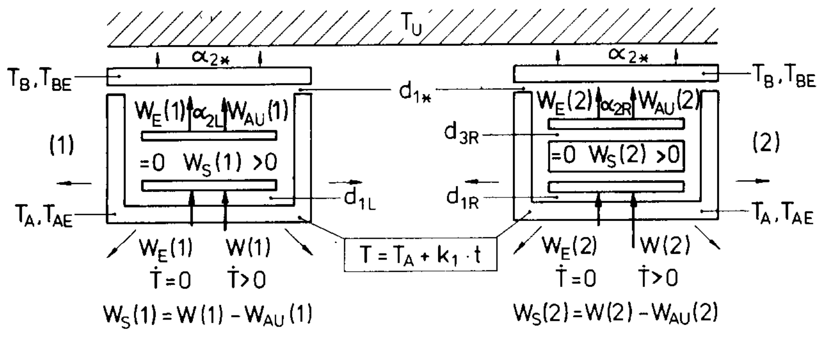

Fig. 1. Model of the differential calorimeter. T_A and T_B are the constant initial temperatures of the sample holder and reference holder and of the sample holder cover and reference holder cover, respectively; α_{2*} and α_2 are heat transfer coefficients; d_{1L}, d_{1R}, d_{3R}, d_{1*} are air gap thicknesses; W_S is the stored heat power, W the power input, and W_{AU} the released heat power. The index R and the label (2) refer to the right side; L and (1) to the left side (reference system).

TABLE 1

Heat coefficients α_2 and α_{2*} for the 100°C and 700°C

T/°C	α_2/W cm^{-2} K^{-1}	α_{2*}/W cm^{-2} K^{-1}
100	1.1×10^{-3}	2.3×10^{-3}
700	3.2×10^{-3}	3.9×10^{-3}

holder and the sample pan, which corresponds to d_{1L} on the left side. The thickness of the air gap between the sample and the sample pan is d_{3R}. The air gap thickness between the sample holder and its cover is identified by d_{1*}, which is also the symbol used for the reference system.

The heat transfer coefficients between the sample pan and the right sample-holder cover and between the reference pan and the left sample-holder cover are α_{2R} and α_{2L}, respectively; the heat transfer coefficients between the covers of the sample holder and the reference holder and the thermostatted cover of the casing are α_{2*} for both sides.

The heat transfer coefficients α_2 and α_{2*} are additive: they comprise radiation, convection and gas heat conduction.

From an average gas flow and with known values of the kinetic viscosity, thermal diffusion and heat conductivity, the Nusselt number can be determined via the Reynolds and Prandtl numbers, using well-known formulae; this number, in turn, is used to determine the convection contribution [5]. The heat transfer coefficients α_2 and α_{2*} for 100 and 700°C were determined together with the heat transport mechanisms for radiation and gas flow, see Table 1.

The sample-holder system with the sample-holder cover represents an indispensible protection of the internal part against heat losses to the surroundings, without which there would be a drastic increase in measuring errors.

Firstly, the sample and reference holder are maintained isothermally at a constant temperature T_A, then heated according to

$$T = T_A + K_1 t$$

with a heating rate of K_1 to a temperature of T_{AE} and again kept constant at this temperature. Depending on the air gap thickness d_{1*} between the sample holder and the sample-holder cover, the sample-holder cover experiences a heating rate K_2, where $K_2 < K_1$; the initial and final temperature on the sample-holder cover are $T_B < T_A$ and $T_{BE} < T_{AE}$, respectively; a representation of the appropriate temperature–time profiles is given in Fig. 2(a) which is also applicable for the reference system. The heating powers required for these temperature programs are shown in Fig. 1. The powers shown on the left side of each system $W_E(1)$ and $W_E(2)$ apply to the isothermal retention range for $T = T_{AE}$; the powers indicated on the

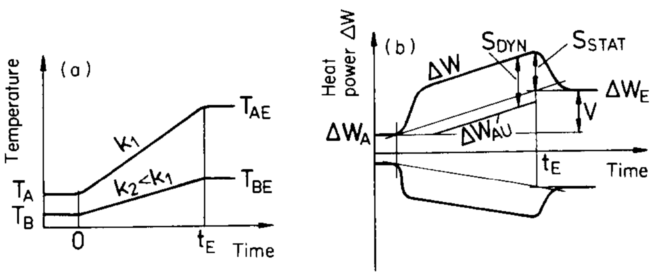

Fig. 2. Graph of the mathematical solution. (a) Temperature behaviour in the sample and reference holder, and the sample holder and reference holder cover, respectively. (b) Static and dynamic heat powers: ΔW is the input power, ΔW_{AU} the release power, ΔW_E the isothermal power input at $T = T_{AE}$, S_{DYN} the dynamic measuring signal, and S_{STAT} the static measuring signal.

right side of each system $W(1)$, $W_S(1)$ and $W_{AU}(1)$, and $W(2)$, $W_S(2)$ and $W_{AU}(2)$, respectively, are for the quasi-stationary range for $T_A < T < T_{AE}$. $W(1)$ and $W(2)$ represent the input power supplied to the internal part of the system; $W_S(1)$ and $W_S(2)$ are the powers stored in the internal part of the system; and $W_{AU}(1)$ and $W_{AU}(2)$ are the powers released from the internal parts of the system.

The following relationships apply to the isothermal phases

$$T = T_A: \quad W = W_A(1) \text{ or } W = W_A(2)$$

$$\Delta W = \Delta W_A = W_A(2) - W_A(1)$$

$$T = T_{AE}: \quad W = W_E(1) \text{ or } W = W_E(2)$$

$$\Delta W = \Delta W_E = W_E(2) - W_E(1)$$

The difference in the power differences for the temperatures T_A and T_{AE} of the right and left system is defined as the offset V.

$$V = \Delta W_E - \Delta W_A$$

Thus, for heating in accordance with the conservation of energy

$$T_A < T < T_{AE}: \quad W(1) = W_S(1) + W_{AU}(1)$$

$$W(2) = W_S(2) + W_{AU}(2)$$

and, thus, for the difference

$$\Delta W = W(2) - W(1) = W_S(2) + W_{AU}(2) - (W_S(1) + W_{AU}(1))$$

$$= \Delta W_S + \Delta W_{AU}$$

with

$$\Delta W_S = W_S(2) - W_S(1)$$

and

$$\Delta W_{AU} = W_{AU}(2) - W_{AU}(1)$$

The powers stored in the heat capacities of the sample and the pan determine the size of the dynamic measuring signal S_{DYN}

$$\begin{aligned} S_{DYN} &= W_S(2) - W_S(1) \\ &= W(2) - W(1) - [W_{AU}(2) - W_{AU}(1)] \\ &= \Delta W - \Delta W_{AU} \end{aligned}$$

In contrast to the steady-state losses ΔE_E, the dynamic losses $\Delta W_{AU} = W_{AU}(2) - W_{AU}(1)$ cannot be determined by measurement; therefore, in addition, it is useful to define the signal quantity

$$S_{STAT} = W(2) - W(1) - \Delta W_E$$

which can be obtained by measurement and for which, as shown later, $S_{DYN} > S_{STAT}$ is always valid, see Fig. 2(b).

MATHEMATICAL SOLUTION

The solutions for the parabolic initial boundary problem, which is of first order, were determined by analysis, and the required parameters K_2 and T_B of the external partial system were computed numerically, assuming constant temperature for the sample and pan.

The following solutions result for the right-hand system

$$W_A(2) = \frac{T_B - T_A}{(1/h_{23})(1 + h_{13}/h_1 + D_1 h_{13}) + 1/h_2 + D_2}$$

$$W_E(2) = \frac{T_{BE} - T_{AE}}{T_B - T_A} W_A(2)$$

$$\begin{aligned} W(2) \;=\; & -(\lambda_1 h_1 K_1/A\{(h_{13}h_{23}c - h_{13}a)z \\ & + (1/a_2)[h_{13}h_{23}(e + scD_1^2/2) - h_{13}b \\ & - sd(D_1 + h_{13}D_1^2/2)]\} - W_A(2)/\lambda_1 + K_2 h_2 h_{13} z/A \end{aligned}$$

$$\begin{aligned} W_{AU}(2) = & -(\lambda_2 h_2 K_2/A\{(gh_{23} - h_{13}h_{23}(1 + h_1 D_1))z \\ & + (1/a_2)[g(D_2 + 0.5h_{23}D_2^2) + srh_{23} \\ & - h_{13}h_{23}[(1 + h_1 D_1)0.5D_2^2 + sv]]\} \\ & + (\lambda_2 h_1 h_{23} K_1/A)h_2 z - W_A(2)/\lambda_2 \end{aligned}$$

where the following symbols and abbreviations are used:

α_2 heat transfer coefficient between the sample pan and the cover of the sample holder, and between the reference pan and the reference holder

α_{2*} heat transfer coefficient between the covers of sample and reference holder, and the isothermal casing

d_1 air gap thickness between sample pan and sample holder, and between reference pan and reference holder

d_{3R} air gap thickness between sample and sample pan

$d_{LR} \approx d_{1R} + d_{3R}$ the total air gap thickness of the sample system (inversely proportional to the total heat transfer coefficient of the heat contacts of the sample side, $\alpha_{KR} \approx 1/d_{LR}$

d_{1*} air gap thickness between sample holder and cover of sample holder, and between the reference holder and cover of the reference holder

D_1 thickness of the reference pan

D_2 thickness of the sample

c_1 specific heat of the sample pan or reference pan

ρ_1 specific gravity of the sample pan or reference pan

λ_1 thermal conductivity of the sample pan or reference pan

c_2 specific heat of the sample

ρ_2 specific gravity of the sample

λ_2 thermal conductivity of the sample ($\lambda_2 = \lambda_P$)

$a_1 = \lambda_1/(\rho_1 c_1)$

$a_2 = \lambda_2/(\rho_2 c_2)$

$h_1 = \alpha_{1R}/\lambda_1$

$h_2 = \alpha_{2R}/\lambda_2$

$h_{13} = \alpha_{3R}/\lambda_1$

$h_{23} = \alpha_{3R}/\lambda_2$

$a = h_2 h_{23} D_2 + h_2 + h_{23}$

$b = D_2 + (h_2 h_{23} D_2^3)/6 + 0.5[(h_2 + h_{23})D_2^2]$

$c = 1 + h_2 D_2$

$d = h_2 h_3 D_2 + h_2 + h_{23}$

$e = 0.5D_2^2 + (h_2 D_2^3)/6$

$g = h_1 h_{13} D_1 + h_1 + h_{13}$

$r = D_1 + (h_1 h_{13} D_1^3)/6 + 0.5[(h_1 + h_{13})D_1^2]$

$s = a_2/a_1$

$A = ga - h_{13}h_{23}(1 + h_1 D_1)$

$E = (1/a_2)[gb - h_{13}h_{23}(1 + h_1 D_1)e]$
$\quad + (1/a_1)[rd - h_{13}h_{23}c(0.5D_1^2 + h_1 D_1^3/6)]$

$z = [(T - T_A)/K_1] - E/A$

The indices R and L refer to the right (sample) and left (reference) systems, respectively.

The parameters used for the computation are

For the sample $c_2 = 0.4\ \mathrm{J\,g^{-1}\,K^{-1}}$, $\rho_2 = 10\ \mathrm{g\,cm^{-3}}$, $D_2 = 1$ mm.

For the aluminium pan $c_1 = 0.88\ \mathrm{J\,g^{-1}\,K^{-1}}$, $\rho_1 = 2.7\ \mathrm{g\,cm^{-3}}$, $D_1 =$ 0.2 mm. The heating rate is $12\ \mathrm{K\,min^{-1}}$.

The air gap thicknesses, heat conductivities and heat transfer coefficients are given in Figs. 4–6 and Table 1.

The use of the parameters is connected with the almost always applicable assumption that the heat transfer coefficients α_2 and α_{2*}, and the air gap thicknesses d_{1*} of the sample and reference system are not essentially different.

The heat powers for the reference system derive from the terms for the sample system given above by determining the limit value with $d_{3R} \rightarrow 0$ and $D_2 \rightarrow 0$.

Figure 2(b) shows the qualitative graph for the computed differences ΔW and ΔW_{AU}, the signal quantities S_{DYN} and S_{STAT}, and the offset V. This graph shows that the power input becomes dependent on time or temperature if the isothermal power ΔW_A at the temperature T_A before heating or the offset v, which is easier to measure, deviate from zero, i.e. if the compensation is easier to measure, deviated from zero, i.e. if the compensation of losses by the reference side is not successful. As shown in the following, the offset may be positive or negative.

The ideal thermal input power ΔW_{ID} is measured if the following is applicable for the static and dynamic state, respectively

$$\Delta W_A = \Delta W_E = V = 0 \quad \text{(static)}$$

$$\Delta W_{AU} = 0 \quad \text{(dynamic)}$$

The deviation of the measuring signal, $S_{DYN} = \Delta W - \Delta W_{AU}$, obtained from the ideal power input, is defined as the dynamic measuring error F, i.e.

$$F = \frac{\Delta W_{ID} - S_{DYN}}{\Delta W_{ID}}$$

If the offset V is referred to the readily measurable static power signal S_{STAT} (see Fig. 2(b))

$$V_1 = \frac{V}{S_{STAT}}$$

a specific offset quantity is obtained which, as shown later, is connected to the measuring error F.

DYNAMIC AND STATIC HEAT LOSSES

In Fig. 3, the difference between the static losses $W_E(2)$ and the dynamic losses $W_{AU}(2)$, referred to the static losses $W_E(2)$, is plotted on the left ordinate against the total heat transfer coefficient α_{KR} and the total air gap thickness d_{LR} of the right system. On the right ordinate, the static losses $W_E(2)$, referred to the ideal power $W_{ID}(2)$, are plotted over the same abscissae.

Large air gap thicknesses and small heat conductivities result in a smaller total conductance, so that, in contrast to the case with minute air gap thicknesses and large heat conductivities, a progressive decrease in the heat powers W_S, W_E, W and W_{AU} occurs in the given sequence, e.g. for W_E, see curves 5 and 7. This means that the power difference $W_E(2) - W_{AU}(2)$ also increases with a reduced total conductance or increases with a growing total air gap thickness d_{LR} (curves 1–4), where a small heat conductivity increases the difference only in the case of good contacts, while poor contacts turn out to be unimportant (curves 1–3). Minor air gap

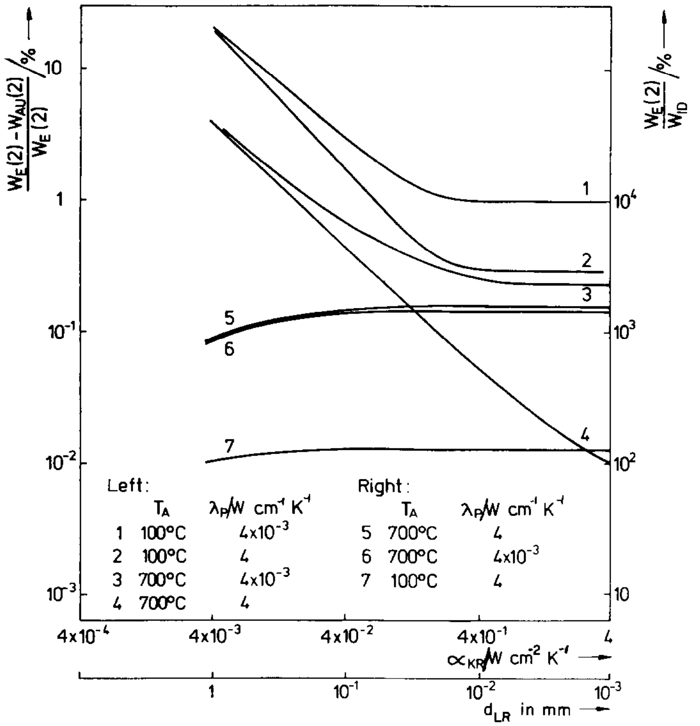

Fig. 3. Dynamic and static heat losses. Left ordinate: the difference is the static and dynamic power losses of the sample system referred to the static power loss; $W_E(2)$ is the static power loss of the sample system, $W_{AU}(2)$ the dynamic power loss of the sample system. Right ordinate: Static losses of the sample system related to the ideal input power of the sample system.

thicknesses and resistances of sample and pan result in a loss difference of around zero, i.e. the static losses agree with dynamic losses, even with a finite heating rate K_1. In this ideal case, in contrast to real cases, the temperature rate gradient and heating rate gradient of the sample and reference system disappears and an exact compensation of losses is produced, i.e. $\Delta W_{AU} = 0$, so that the following is valid

$$\Delta W = \Delta W_S = \Delta W_{ID}$$

Hence, under these ideal conditions the obtained difference signal of the power output is in exact agreement with the ideal power input of the sample.

DYNAMIC ERRORS AND SPECIFIC OFFSET

Figures 4–6 show the dynamic error $F = (\Delta W_{ID} - S_{DYN})/\Delta W_{ID}$ as a function of the specific offset V_1 for various temperatures and air gap thicknesses d_{1L}, $d_{LR}(\approx d_{1R} + d_{3R})$ and d_{1*}. The parameter of the curves is the thickness d_{1L} of the air gap between the reference sample holder and the reference pan. Each curve is represented as a geometric locus for the total contact heat transfer coefficient α_{KR} of the sample system, where all curves begin at strongly negative offsets V_1 with the same total contact heat transfer coefficient $\alpha_{Kr} = 3.6 \times 10^{-3}\ \mathrm{W\,cm^{-2}\,K^{-1}}$, which is equivalent to a total air gap thickness d_{LR} of 1 mm. With smaller air gap thicknesses d_{LR} between the reference sample holder and the reference pan, the α_{KR} values

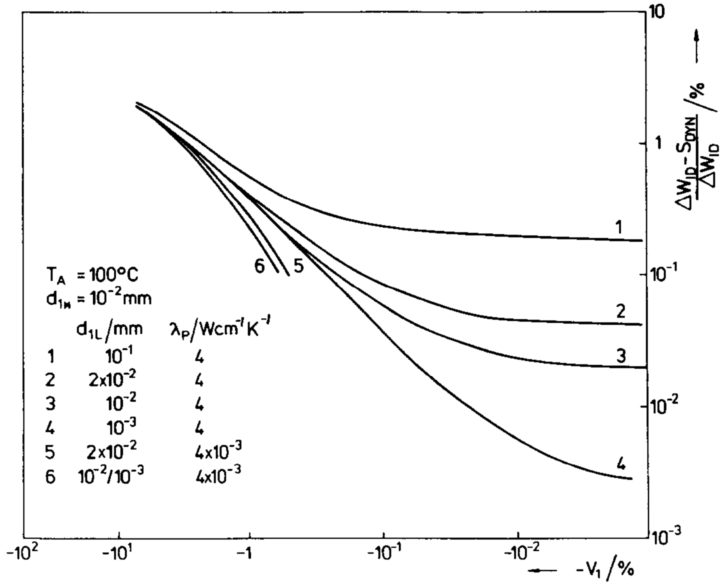

Fig. 4. Dynamic error $F = (\Delta W_{ID} - S_{DYN})/\Delta W_{ID}$ as a function of the specific offset V_1 for 100°C, $d_{1*} = 10^{-2}$ mm, and $\lambda_2 = 4$ and $4 \times 10^{-3}\ \mathrm{W\,cm^{-1}\,K^{-1}}$.

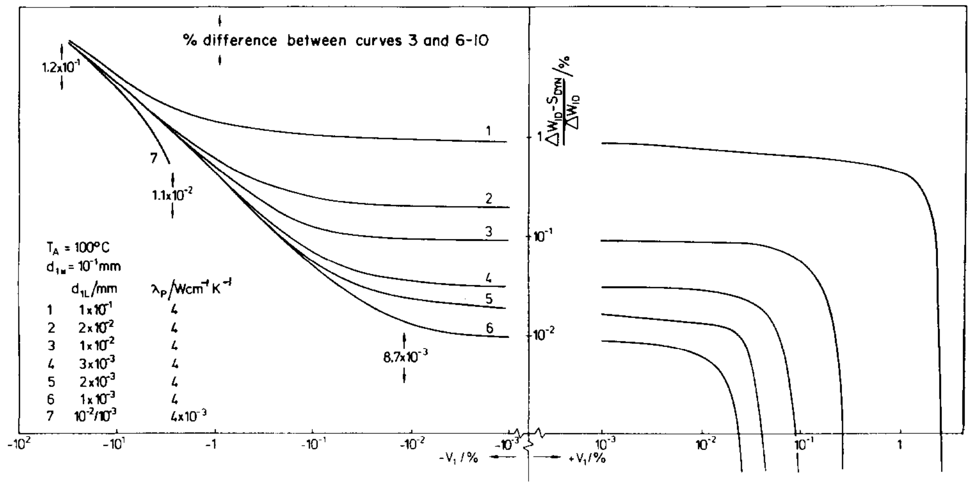

Fig. 5. Dynamic error $F = (\Delta W_{ID} - S_{DYN})/\Delta W_{ID}$ as a function of the specific offset V_1 for 100°C, $d_{1*} = 10^{-1}$ mm, and $\lambda_2 = 4$ and 4×10^{-3} W cm^{-1} K^{-1}.

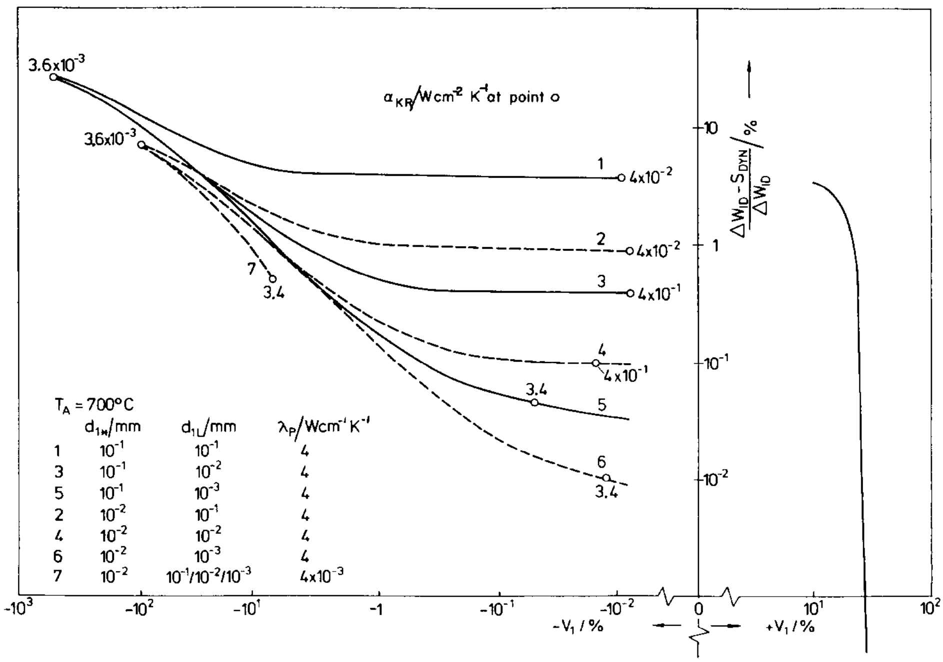

Fig. 6. Dynamic error $F = (\Delta W_{ID} - S_{DYN})/\Delta W_{ID}$ as a function of the specific offset V_1 for 700°C, $d_{1*} = 10^{-1}$ mm and 10^{-2} mm, and $\lambda_2 = 4$ and 4×10^{-3} W cm^{-1} K^{-1}.

TABLE 2

Relation between the signs of the isothermal differential heat power ΔW_E, specific offset V_1, the dynamic error F and the difference between the total air gap thickness d_{LR} for the sample side and the air gap thickness d_{1L} of the reference side

$d_{LR} - d_{1L}$	W_E	V_1	$F = \frac{\Delta W_{ID} - S_{DYN}}{\Delta W_{ID}}$
>0	<0	<0	>0
⩽0	⩾0	⩾0	⩾/⩽0

are shifted closer together on the corresponding curve, so that for $d_{1*} = 10^{-2}$ mm, $d_{1L} = 10^{-3}$ mm and $\lambda_2 = 4\ \text{W cm}^{-1}\ \text{K}^{-1}$ (curve 6 in Fig. 6) at $V_1 = -10^{-2}\%$, the value $\alpha_{KR} = 3.4\ \text{W cm}^{-2}\ \text{K}^{-1}$ or $d_{LR} = 10^{-3}$ mm is obtained; in curve 2 ($d_{1L} = 10^{-1}$ mm) with the same V_1, only $\alpha_{KR} = 4 \times 10^{-2}\ \text{W cm}^{-2}\ \text{K}^{-1}$ or $d_{LR} = 0.1$ mm is valid.

The curves show negative and positive values for the offsets V_1 and the dynamic errors F. They are caused by the differences in the total air gap thicknesses d_{LR} and d_{1L} of the sample and reference side, respectively. This is shown in Table 2.

Because it seems unlikely that the total air gap thickness d_{LR} of the sample system is less than the air gap thickness d_{1L} of the reference system, positive offsets V_1 will rarely be observed. Positive offsets errors are only created with $F \leqslant 0$.

Figures 4–6 indicate that the dynamic errors F increase, as expected, with growing air gap thicknesses between the sample holder or reference holder and the pan, between pan and sample, between sample holder or reference holder and the covers of sample holder and reference holder and, of course, with higher temperatures. Curves 1, 2 and 4 in Fig. 6, for instance, show a drastic decrease in the minimal error from 5% to 0.1% if all air gap thicknesses are reduced from 0.1 to 0.01 mm.

Because, however, the exact air gap thicknesses and heat transfer coefficients are not known, a clear assignment of errors to the specific offset V_1 is desirable as the latter is readily determined. This is possible if good heat contact between the reference pan and the reference sample holder is provided on the reference side. Then, depending on the contact, the upper curves, which most of all contribute to an ambiguous dependence of the error F on the specific offset V_1, well no longer be applicable. The residual ambiguity in the lower range of errors is practically unimportant if the air gap thicknesses between the sample holder or reference holder and the cover of the sample holder or reference holder, respecitively, are smaller than 0.1 mm, which is usually the case under practical conditions.

Table 3 shows that in these cases, even at 700°C, the ranges of ambiguity are about $\Delta F \leqslant 0.1\%$, i.e. they are unimportant from a practical point of view.

TABLE 3

Maximum ambiguity ΔF of the dynamic error F with small specific offsets V_1 for $d_{1*} \leq 0.1$ mm

T/°C	d_{1L}/mm	d_{1*}/mm	F%	Figure
100	$\leq 10^{-2}$	$\leq 1 \times 10^{-2}$	$\leq 2 \times 10^{-2}$	4
100	$\leq 10^{-2}$	$\leq 1 \times 10^{-1}$	$\leq 1 \times 10^{-1}$	5
700	$\leq 10^{-2}$	$\leq 1 \times 10^{-2}$	$\leq 1 \times 10^{-1}$	6
700	$\leq 10^{-2}$	$\leq 1 \times 10^{-1}$	$\leq 4 \times 10^{-1}$	6

The error curves shown in Figs. 4–6 are valid for heat conductivities that differ by three orders of magnitude, where the given heat conductivities of 4 and 4×10^{-3} W cm^{-1} K^{-1} were used.

For all heat conductivities, the error curves for increasing negative specific offsets V_1 coincide more and more, because with poor heat contacts on the reference and sample side, the influence of the heat conductivity can be generally neglected.

Smaller conductivities of the sample result in smaller ranges of the error curve, because in this case even with very small air gap thicknesses, smaller errors cannot be obtained, i.e. a lower error limit is established. This case is represented by curves 5 and 6 in Fig. 4, and curve 7 in Figs. 5 and 6.

If the error curves for all temperatures and contacts, with rejection of air gap thicknesses above 0.1 mm between the reference sample holder and reference pan, are plotted together against the negative specific offset, the curve behaviour of Fig. 7 is obtained which, independent of the heating

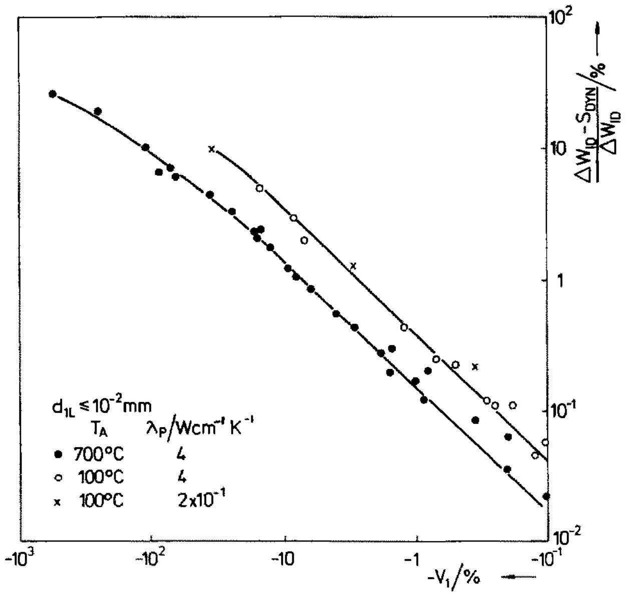

Fig. 7. Dynamic error $F = (\Delta W_{ID} - S_{DYN})/\Delta W_{ID}$ as a function of the specific offset V_1 for all temperatures; d_{1*} and λ_2 values for small air gap thicknesses only ($d_{1L} \leq 0.01$ mm).

rate, heat conductivity and heat capacity of the sample, provides a sufficiently explicit correspondence between the error and specific offset.

CONCLUSIONS

This study indicates that the air gaps in all parts of an isoperibolic DSC apparatus entail essential measuring errors. These errors were determined exactly with respect to the temperature, air gap thickness, thermophysical properties of the sample and process parameters. However, these quantities are mostly unknown, so that these computations are only important in the qualitative consideration of errors. To enable the determination of quantitative errors, the non-compensated dynamic heat losses can be attributed, by means of specific offsets, to static losses. If air gap thicknesses above 0.1 mm between the reference sample holder and the reference pan are rejected, the dynamic measuring errors can be adequately represented as a function of the negative specific offset. Assuming identical heat transfer coefficients α_2 and α_{2*} in the sample and reference system, which, actually, is mostly valid, the errors can be determined as a function of the specific offset with sufficient explicitness. With smaller air gap thicknesses between the reference sample holder and the reference pan, the error values also become smaller (with an air gap thickness d_{1*} of 0.1 mm, to $F = 0.1\%$, and with an air gap thickness d_{1*} of 0.05 mm, to $F = 10^{-2}\%$).

Because, on principle, the reference pan can always be left in the reference holder and, in contrast to the sample pan, is not subject to unexpected changes, careful positioning should be possible. Then the measuring errors caused by geometric and emission-related changes of the sample and the sample pan can be easily determined as a function of the specific offset V_1, without knowing the details of these changes. If the constant-temperature air gaps and heat contact conditions assumed for the determination are not valid under practical conditions, the defined specific offset V_1 should be replaced by the static differential losses ΔW_A and ΔW_E before and after heating to assess the dynamic error. The determination of these static losses instead of V_1 is only inconvenient if digital storage of signals is not possible, a case which rarely occurs nowadays.

REFERENCES

1 W. Hemminger and G. Höhne, Grundlagen der Kalorimetrie, Verlag Chemie, Weinheim, New York, 1979.
2 W. Poeßnecker, J. Therm. Anal. 36 (1990) 1123–1139.
3 W. Poeßnecker, Thermochim. Acta, 187 (1991) 309–322.
4 W. Poeßnecker, Thermochim. Acta, 219 (1993) 325.
5 F. Hell, Grundlagen der Wärmeübertragung, VDI-Verlag, Düsseldorf, 1982.